High-resolution live-cell imaging reveals novel cyclin A2 degradation foci involving autophagy

Abdelhalim Loukil, Manuela Zonca, Cosette Rebouissou, Véronique Baldin, Olivier Coux, Martine Biard-Piechaczyk, Jean-Marie Blanchard, Marion Peter

© 2014. Published by The Company of Biologists Ltd | Journal of Cell Science (2014) 127, 2145–2150 doi:10.1242/jcs.139188

SHORT REPORT

High-resolution live-cell imaging reveals novel cyclin A2 degradation foci involving autophagy

Abdelhalim Loukil[1], Manuela Zonca[1], Cosette Rebouissou[1], Véronique Baldin[2], Olivier Coux[2], Martine Biard-Piechaczyk[3], Jean-Marie Blanchard[1] and Marion Peter[1,*]

ABSTRACT

Cyclin A2 is a key player in the regulation of the cell cycle. Its degradation in mid-mitosis relies on the ubiquitin-proteasome system (UPS). Using high-resolution microscopic imaging, we find that cyclin A2 persists beyond metaphase. Indeed, we identify a novel cyclin-A2-containing compartment that forms dynamic foci. Förster (or fluorescence) resonance energy transfer (FRET) and fluorescence lifetime imaging microscopy (FLIM) analyses show that cyclin A2 ubiquitylation takes place predominantly in these foci before spreading throughout the cell. Moreover, inhibition of autophagy in proliferating cells induces the stabilisation of a subset of cyclin A2, whereas induction of autophagy accelerates the degradation of cyclin A2, thus showing that autophagy is a novel regulator of cyclin A2 degradation.

KEY WORDS: FLIM, FRET, Autophagy, Cyclin A2, Mitosis, Ubiquitin-proteasome system

INTRODUCTION

Cyclin-dependent kinases (Cdk), which govern progression through the cell cycle, are mainly controlled by transient interactions with cyclins and by reversible phosphorylation (Morgan, 1997). Cyclin A2 activates Cdk1 and Cdk2, and hence regulates both S phase and mitosis (Pagano et al., 1992). It is also involved in cell invasion (Arsic et al., 2012).

Cyclin A2 accumulates from late G1 to M phase and is degraded by the ubiquitin-proteasome system (UPS) (Sudakin et al., 1995) before metaphase (den Elzen and Pines, 2001; Geley et al., 2001). Cyclin A2 is ubiquitylated by the anaphase-promoting complex (also called the 'cyclosome', APC/C), which is activated by cell-division cycle protein 20 (Cdc20). The degradation of cyclin A2 is also regulated by acetylation (Mateo et al., 2009). Cyclin A2 proteolysis is required for chromosome alignment and anaphase progression (den Elzen and Pines, 2001). Moreover, cyclin A2 degradation is independent of the spindle-assembly checkpoint (Di Fiore and Pines, 2010; Izawa and Pines, 2011; Wolthuis et al., 2008).

[1]Institut de Génétique Moléculaire de Montpellier, CNRS, Université Montpellier 2, Université Montpellier 1, 1919 route de Mende, 34293 Montpellier, France. [2]Centre de Recherche de Biochimie Macromoléculaire, CNRS, Université Montpellier 2, Université Montpellier 1, 1919 route de Mende, 34293 Montpellier, France. [3]Centre d'étude d'agents Pathogènes et Biotechnologies pour la Santé, CNRS, Université Montpellier 2, Université Montpellier 1, 1919 route de Mende, 34293 Montpellier, France.

*Author for correspondence (marion.peter@igmm.cnrs.fr)

Received 26 July 2013; Accepted 21 February 2014

Here, we have analysed the intracellular distribution of the ubiquitylated forms of cyclin A2, using high resolution microscopic imaging, notably FRET (Förster or fluorescence resonance energy transfer) and FLIM (fluorescence lifetime imaging microscopy). These non-invasive and quantitative techniques allow the detection of protein interactions at the subcellular level in live cells, producing data that are highly resolved in time and space (Peter and Ameer-Beg, 2004; Peter et al., 2005). The ubiquitylated forms of cyclin A2 accumulate in dynamic foci located at the periphery of mitotic cells. We also find a role for autophagy, as pharmacological inhibition and shRNA-mediated knockdown of autophagy-related protein 7 (Atg7) both stabilise a proportion of cyclin A2. By contrast, induction of autophagy by starvation accelerates cyclin A2 breakdown, thus implicating autophagy as an additional pathway for the degradation of cyclin A2.

RESULTS AND DISCUSSION

Cyclin A2 ubiquitylation occurs predominantly in foci

We investigated cyclin A2 ubiquitylation by using FRET measured by FLIM. Synchronised MCF-7 cells were microinjected with vectors encoding cyclin-A2–EGFP and either ubiquitin–mCherry or mCherry alone. In prometaphase, we observed FRET between cyclin-A2–EGFP and ubiquitin–mCherry essentially in foci (Fig. 1A, upper panels), where the decrease of EGFP fluorescence lifetime due to FRET was significant (from 2.01 ns to 1.82 ns, Fig. 1B, upper panel). As a negative control, we generated a mutant where all but five lysines were changed to arginine (cyclin-A2-K5). The conserved lysines (K168, K266, K288, K289 and K412) lie at the interface with Cdk. Cyclin-A2-K5–EGFP remained detectable throughout mitosis (supplementary material Fig. S1A). Despite its abundance at metaphase, we did not detect FRET between cyclin-A2-K5–EGFP and ubiquitin–mCherry, whereas FRET occurred between the wild-type cyclin-A2-wt–EGFP and ubiquitin–mCherry in foci and elsewhere in cells (Fig. 1A, lower panels; Fig. 1B, lower panel). Thus, cyclin A2 ubiquitylation occurs mainly in foci in prometaphase and spreads throughout the cell during metaphase.

Importantly, the foci were readily detected when imaging cyclin-A2–EGFP alone, following microinjection of the expression vector (Fig. 1C, left panel, row 1) or stable transfection with an inducible vector (Fig. 1C, left panel, row 2), a novel observation to our knowledge. The subcellular localisation of cyclin A2 has previously been characterised in different cell lines using microscopy. It is predominantly nuclear (Bailly et al., 1992; Dulić et al., 1998; Pagano et al., 1992; Pines and Hunter, 1991) and shuttles between the nucleus and cytoplasm (Jackman et al., 2002). Cyclin A2 distribution is diffuse during mitosis and interphase, apart from dots corresponding to replication foci (Cardoso et al., 1993; Sobczak-Thepot et al., 1993) and centrosomes (Bailly et al.,

Journal of Cell Science (2014) 127, 2145–2150 doi:10.1242/jcs.139188

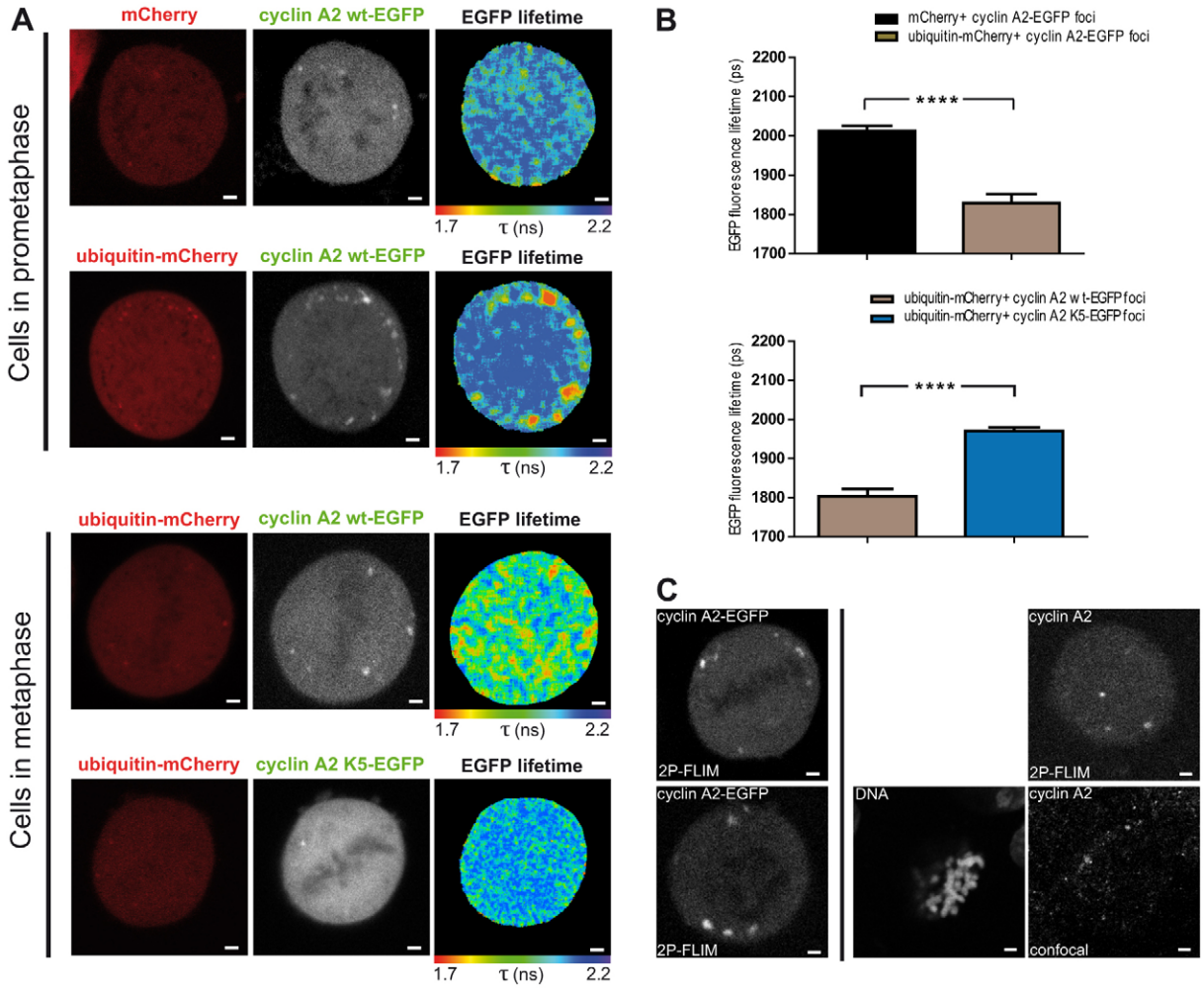

Fig. 1. Cyclin A2 ubiquitylation occurs predominantly in foci. (A) Upper panels, live MCF-7 cells microinjected with pEGFP-N1-cyclin-A2 and pmCherry-C1 or pmCherry-C1-ubiquitin. Lower panels, live MCF-7 cells microinjected with wild-type (wt) or K5-mutant pEGFP-N1-cyclin-A2 and pmCherry-C1-ubiquitin. $n>100$ cells. (B) Data represent the mean±s.e.m. of cyclin-A2–EGFP foci lifetimes under the conditions shown in A. Upper panel: mCherry+cyclin-A2-wt–EGFP ($n=24$), ubiquitin–mCherry+cyclin-A2-wt–EGFP ($n=28$). Lower panel: ubiquitin–mCherry+cyclin-A2-wt–EGFP ($n=20$), ubiquitin–mCherry+cyclin-A2-K5–EGFP ($n=30$). ****$P<0.0001$. (C) Left, row 1, a live MCF-7 cell microinjected with pEGFP-N1-cyclin-A2; row 2, a live U2OS cell induced to express cyclin-A2–EGFP. Right, MCF-7 cells were fixed and immunostained for endogenous cyclin A2; row 1, image obtained by two-photon excitation with a FLIM detector; row 2, confocal images showing DNA (left) and cyclin A2 (right). Scale bars: 2 μm.

1992; Pascreau et al., 2010). *A priori*, neither of these corresponds to the foci that we observed. Cyclin-A2–EGFP has proven to be a valuable tool that reflects faithfully its endogenous counterpart (den Elzen and Pines, 2001; Di Fiore and Pines, 2010; Jackman et al., 2002; Walker et al., 2008; Wolthuis et al., 2008). To avoid artefacts, we have established experimental conditions to express cyclin-A2–EGFP at low levels (supplementary material Fig. S1B). Whenever possible, we confirmed that cells underwent mitosis and cytokinesis with kinetics similar to those of controls (supplementary material Fig. S1C). We performed acquisitions by time-domain FLIM of MCF-7 cells immunostained for endogenous cyclin A2. We used two-photon excitation, keeping photobleaching to a minimum. By accumulating photons through time, we actually detected several foci in mitotic cells (Fig. 1C, right panel, row 1). Detection of foci using confocal microscopy was difficult (Fig. 1C, right panel, row 2), only being possible with the latest generation detectors, e.g. gallium-arsenide-phosphide (GaAsP) photomultiplier tubes (PMT). These observations show that cyclin-A2-rich foci do indeed exist during mitosis.

Dynamics of cyclin-A2-rich foci

We used cyclin-A2–EGFP to better characterise the dynamics of the foci during mitosis. Synchronised MCF-7 cells were microinjected with the cyclin-A2–EGFP expression plasmid as above. Cyclin-A2-rich foci were observed between prometaphase and telophase (Fig. 2A; supplementary material Fig. S2A). They localised mainly at the periphery of the cells and moved in three dimensions (supplementary material Movie 1). Cyclin-A2–EGFP intensity decreased through mitosis because of degradation, but remained higher in foci (Fig. 2A, graph). Similar foci were observed in microinjected MCF-10A and MDA-MB-231 cells, and in U2OS cells stably transfected with an inducible expression vector (supplementary material Fig. S2A). Endogenous cyclin A2 was quantified beyond prometaphase (supplementary material Fig. S2B), following a nocodazole block (Thomas et al., 2010). Our observations show that a fraction of cyclin A2 persists later in mitosis than described previously, with a particular localisation in foci. Moreover, certain foci contain ubiquitylated cyclin A2, suggesting that they might correspond to sites of cyclin A2 degradation (Seeger et al., 2003).

Journal of Cell Science (2014) 127, 2145–2150 doi:10.1242/jcs.139188

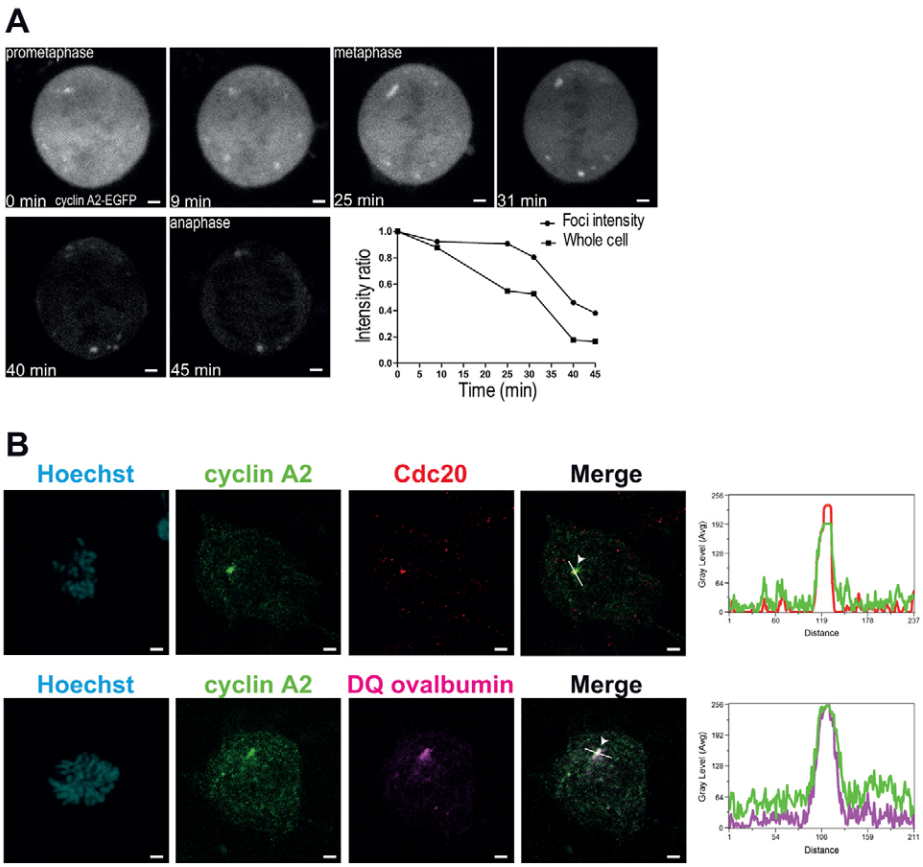

Fig. 2. Dynamics of cyclin-A2-rich foci. (A) An MCF-7 cell microinjected with pEGFP-N1-cyclin-A2. Two-photon images are shown. The data shown in the graph represent the mean intensity relative to t_0 (prometaphase). (B) Confocal images. Upper panel, MCF-7 cells were fixed and immunostained for cyclin A2 and Cdc20 [$n=33$ (89% positive)]. Lower panel, MCF-7 cells were microinjected with DQ ovalbumin and immunostained for cyclin A2 [$n=34$ (100% positive)]. Spectral colocalisation plots of the indicated foci (white arrowheads and lines) are shown to the right. Green, cyclin A2; Red, Cdc20; Pink, DQ ovalbumin. Scale bars: 2 µm.

Indeed, during prometaphase, we visualised the colocalisation of endogenous cyclin A2 with Cdc20, a key regulator of cyclin A2 ubiquitylation. Cdc20 staining was punctate as described previously (Kallio et al., 1998), but also colocalised with cyclin A2 in several foci (Fig. 2B). Furthermore, a few cyclin A2 foci colocalised with active proteasomes, which were identified by the rapid digestion of microinjected DQ ovalbumin (Fig. 2B) (Baldin et al., 2008; Rockel et al., 2005). Cdk binding is required for the correct timing of cyclin A2 degradation (den Elzen and Pines, 2001), and Cdks are likely to be associated with cyclins when the latter are degraded by the proteasome (Nishiyama et al., 2000). Indeed, we detected FRET between cyclin-A2–EGFP and Cdk1–mCherry in foci and elsewhere in MCF-7 cells during mitosis (supplementary material Fig. S2C).

Thus, some foci could be sites of both ubiquitylation and proteasomal degradation of cyclin A2. Nevertheless, not all cyclin A2 foci colocalised with Cdc20 or DQ ovalbumin. Furthermore, cyclin A2 foci persist until late mitosis, i.e. after most proteasomal degradation of cyclin A2 has occurred. We therefore hypothesised that cyclin A2 degradation might involve another pathway.

Autophagy also mediates cyclin A2 degradation

Autophagy is a major pathway for intracellular proteolysis, so we investigated its contribution to cyclin A2 degradation. First, we used bafilomycin A1 (BFA), a lysosomal proton-pump inhibitor that inhibits the autophagosome–lysosome fusion step and autophagy flux (Yamamoto et al., 1998; Yoshimori et al., 1991). In MCF-7 cells treated with BFA, some endogenous cyclin A2 foci colocalised with light chain 3-B protein (LC3-B), a marker of autophagosomes, during metaphase (Fig. 3A, row 1). We also detected colocalisation of some cyclin A2 foci with p62 (also known as SQSTM1; Fig. 3A, row 2), a receptor for ubiquitylated proteins that is necessary for their degradation by selective autophagy (Pankiv et al., 2007) and is stabilised by BFA treatment (Bjørkøy et al., 2005; supplementary material Fig. S3A). We used LysoTracker to detect colocalisation of cyclin A2 with lysosomes. Because LysoTracker exhibits faint fluorescence in fixed cells, we used live MCF-7 cells ectopically expressing cyclin-A2–EGFP without BFA treatment. Many cyclin-A2–EGFP foci colocalised with lysosomes (Fig. 3A, row 3). Note that there is stronger colocalisation between cyclin-A2–EGFP and LC3-B–mCherry under the same conditions (supplementary material Fig. S3B). Consistent with these observations, endogenous cyclin A2 co-immunoprecipitated with LC3-B and with p62 from MCF-7 cells synchronised in G2/M (Fig. 3B), but not in G1/S (supplementary material Fig. S3C).

Moreover, no colocalisation between cyclin A2 and LC3-B, p62 or lysosomes was detected at the beginning of prometaphase, whereas no colocalisation between cyclin A2 and Cdc20 or DQ ovalbumin was observed during metaphase. This suggests that, in prometaphase, cyclin A2 foci colocalised mainly with Cdc20 or DQ ovalbumin, whereas in metaphase, they colocalised mainly with LC3-B, p62 or lysosomes. Thus, we think that autophagy-mediated cyclin A2 degradation occurs later in the cell cycle than UPS-mediated degradation, with, at best, partial overlap between the two mechanisms. Colocalisation between cyclin A2, DQ ovalbumin and LC3-B was rarely detected in the same cells. Importantly, when this occurred, i.e. in late prometaphase, foci containing endogenous cyclin A2 colocalised with either LC3-B or DQ ovalbumin (Fig. 3A, row 4). This suggests that there are two distinct populations of these foci, linked to one pathway or the other.

Journal of Cell Science (2014) 127, 2145–2150 doi:10.1242/jcs.139188

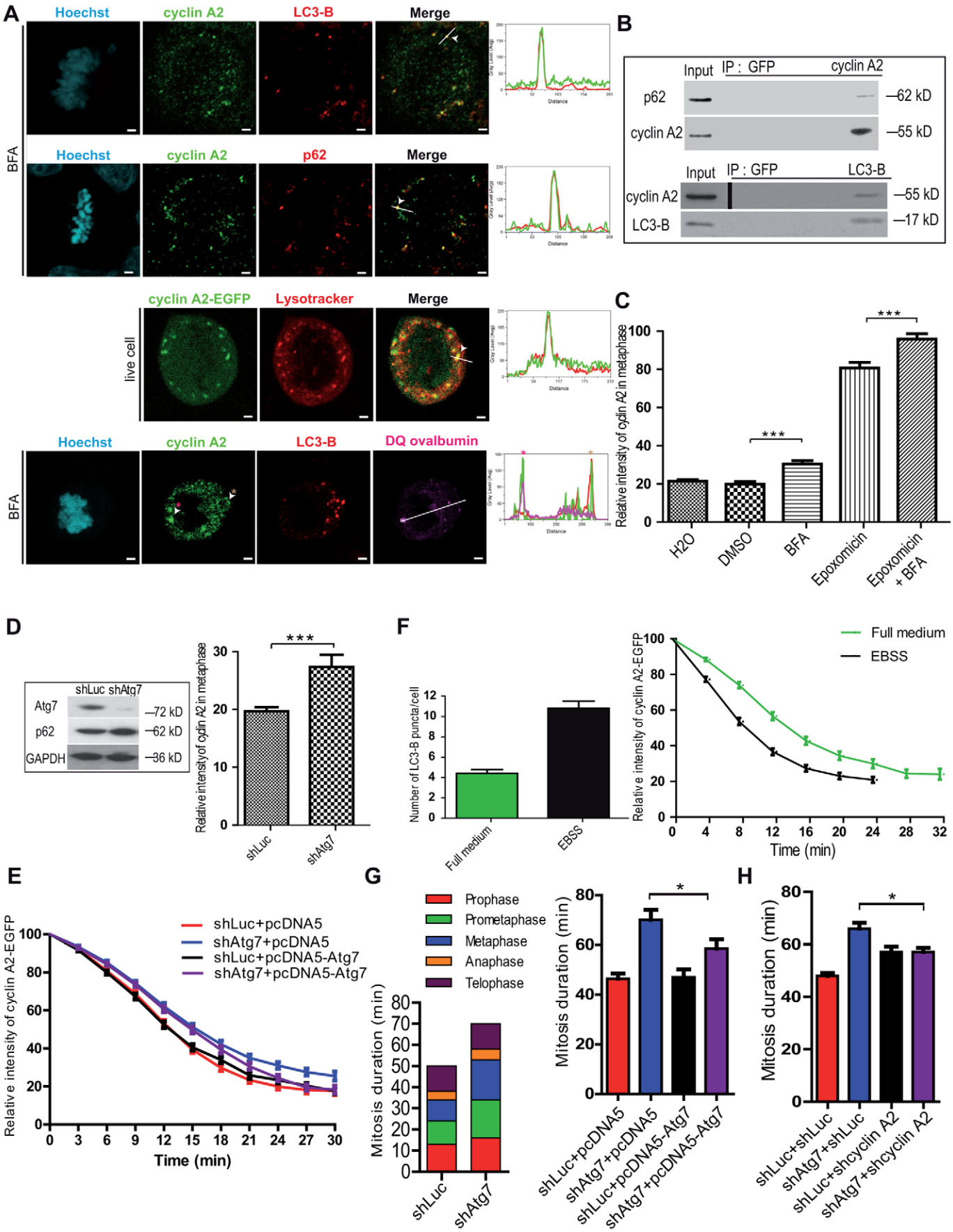

Fig. 3. See next page for legend.

Fig. 3. Autophagy also mediates the degradation of cyclin A2. (A) Rows 1, 2 and 4 show BFA-treated fixed MCF-7 cells. Row 1, cells were immunostained for cyclin A2 and LC3-B [*n*=43 (96% positive)]; row 2, cells were immunostained for cyclin A2 and p62 [*n*=24 (96% positive)]; row 3, live MCF-7 cells were microinjected with pEGFP-N1-cyclin-A2 and stained with LysoTracker (*n*=7); row 4, cells were microinjected with DQ ovalbumin and immunostained for cyclin A2 and LC3-B (*n*=5). Spectral colocalisation plots of the indicated foci (white arrowheads and lines) are shown to the right. Asterisks indicate two particular foci displaying colocalisation with either DQ ovalbumin or LC3-B. Scale bars: 2 μm. (B) Immunoprecipitation (IP) from G2/M MCF-7 cells. Black bar distinguishes two exposures of same immunoblot. (C) Synchronised MCF-7 cells were treated with DMSO, BFA and/or epoxomicin, fixed and immunostained for cyclin A2. Data depict the mean intensity of cyclin-A2–EGFP in metaphase relative to the mean intensity in interphase (±s.e.m.). H_2O, *n*=38; DMSO, *n*=54; BFA, *n*=111; epoxomicin, *n*=82; BFA+epoxomicin, *n*=124. ***$P<0.0003$. (D) MCF-7 cells were infected with retrovirus carrying shRNA against luciferase or Atg7, synchronised, fixed and immunostained for cyclin A2. Left, immunoblot showing Atg7 and p62 levels. Right, graph showing cyclin A2 levels in metaphase, as in C. ShLuc, *n*=64; shAtg7, *n*=43. ***$P<0.0005$. (E) Cells of the U2OS-cyclin-A2-EGFP inducible cell line were infected with retrovirus carrying shRNA against luciferase or Atg7, transfected with pcDNA5 or pcDNA5-Atg7, induced to express cyclin-A2–EGFP and followed by time-lapse imaging. t_0, prophase. The intensity of cyclin-A2–EGFP was quantified relative to t_0. Data represent the mean±s.e.m. *n*=42. (F) U2OS cells were induced to express cyclin-A2–EGFP and were incubated in full medium or EBSS for 12 h. Left, quantification of LC3-B puncta in mitotic cells (*n*=30). Right, quantification of cyclin-A2–EGFP intensity. t_0, prophase. Full medium, *n*=29; EBSS, *n*=31. (G) Left, duration of mitotic stages measured from time-lapse imaging performed with asynchronous U2OS cells that were infected with retrovirus carrying shRNA against luciferase or Atg7. The data represent the means from shLuc (*n*=118) and shAtg7 (*n*=110) cells. The results obtained for prophase, prometaphase, metaphase and anaphase are significantly different ($P<0.0001$). Right, the duration of mitosis measured from time-lapse imaging of the U2OS-cyclin-A2-EGFP inducible cell line, infected with retrovirus carrying shRNA against luciferase or Atg7 and transfected with pcDNA5 or pcDNA5-Atg7. Data represent the mean±s.e.m. from shLuc+pcDNA5 (*n*=102), shAtg7+pcDNA5 (*n*=100), shLuc+pcDNA5-Atg7 (*n*=107), shAtg7+pcDNA5-Atg7 (*n*=62). *$P=0.0391$. (H) The duration of mitosis was measured by time-lapse imaging of U2OS cells that were infected sequentially with retrovirus carrying shRNA against luciferase and Atg7 or cyclin A2. Data represent the mean±s.e.m. from shLuc+shLuc (*n*=111), shAtg7+pcLuc (*n*=101), shLuc+shcyclin-A2 (*n*=105) and shAtg7+shcyclin-A2 (*n*=83). *$P=0.0141$.

To estimate the relative contributions of UPS versus autophagy to cyclin A2 degradation, synchronised MCF-7 cells were treated with epoxomicin (a proteasome inhibitor) and/or BFA. Immunofluorescence-based quantification of endogenous cyclin A2 in metaphase cells showed a significant increase in the level of the protein after either treatment, although that seen with BFA was lower than the increase observed with epoxomicin (Fig. 3C). Thus, both pathways contribute to cyclin A2 degradation. The additive effect of the two inhibitors (Fig. 3C) further suggests that the two pathways function in parallel.

To confirm the contribution of autophagy to cyclin A2 degradation, we used a shRNA directed against autophagy-related protein 7 (Atg7), an E1-like activating enzyme required for autophagosome formation (Tanida et al., 2001). We then evaluated the level of endogenous cyclin A2 in metaphase cells. Atg7 shRNA expression led to increased p62 levels in MCF-7 cells (Fig. 3D; supplementary material Fig. S3D) and increased cyclin A2 levels in metaphase (Fig. 3D). These data are consistent with a role for autophagy in cyclin A2 degradation.

We used U2OS cells with inducible expression of cyclin-A2–EGFP to study its degradation by time-lapse microscopy. In the presence of the Atg7 shRNA expression vector, cells displayed slower cyclin A2 degradation (Fig. 3E; supplementary material Fig. S3D, Movies 2, 3). Notably, this phenotype was partially rescued by expressing an shRNA-resistant version of Atg7 (Fig. 3E).

Inducing autophagy by starving U2OS cells expressing cyclin-A2–EGFP led to a 2.5-fold increase in the number of LC3-B puncta detected by immunofluorescence (Fig. 3F, left panel). Under these conditions, cyclin-A2–EGFP was degraded more rapidly than in non-starved cells (Fig. 3F, right panel), further confirming that autophagy contributes to cyclin A2 degradation. Inhibition of autophagy by Atg7 shRNA led to prolonged mitosis in U2OS cells (Fig. 3G) and in MCF-7 cells (supplementary material Fig. S3E). In particular, prometaphase and metaphase were delayed (Fig. 3G, left panel), consistent with effects on cyclin A2 degradation (den Elzen and Pines, 2001). Again, this defect was partially rescued by expressing shRNA-resistant Atg7 (Fig. 3G, right panel). We investigated whether the mitotic delay observed in Atg7-shRNA-treated (shAtg7) cells was a consequence of the partial stabilisation of cyclin A2. U2OS cells were treated sequentially with Atg7 shRNA and with cyclin A2 shRNA. Cells proceeded through and completed M phase, in spite of treatment with cyclin A2 shRNA. The mitotic delay in shAtg7 cells was partially rescued by treatment with cyclin A2 shRNA (the duration of mitosis in shAtg7+shLuc cells was 65.9 min; in shAtg7+shcyclin-A2 cells it was 57.1 min and in shLuc+shcyclin-A2 cells it was 57.2 min; Fig. 3H; supplementary material Fig. S3F). The increase in mitotic duration in cyclin-A2-depleted cells compared with control cells has already been described by our laboratory (Arsic et al., 2012) and by others (Fung et al., 2007). Our results suggest that autophagy inhibition induces a mitotic delay that is a consequence of the partial stabilisation of cyclin A2.

Autophagy, characterised as a recycling process for defective structures, is progressively being implicated in regular cellular catabolic pathways. We propose that autophagy plays a role in the degradation of cyclin A2 as a complementary mechanism to prevent its accumulation at the end of mitosis.

MATERIALS AND METHODS

Constructs

Human cyclin A2 cDNA was subcloned into pEGFP-N1 (Clontech); ubiquitin, Cdk1 and LC3-B cDNAs were subcloned into pmCherry-C1 (Tramier et al., 2006); and Atg7 cDNA was subcloned into pcDNA5/FRT-HA (Invitrogen). The cyclin-A2-K5 mutant was synthesised by GenScript. Retroviruses were generated with pLKO.1-Luciferase-shRNA (SHC007, Sigma-Aldrich), pLKO.1-shAtg7 (TRCN0000007584, Sigma-Aldrich) or pSIREN-RetroQ (cyclin-A2-targeting sequence, 5′-GTAGCAGAGTTTGTGTATA-3′).

Cell culture and treatments

MCF-7 cells were grown in RPMI (Gibco) supplemented with 10% FBS (PAA). The U2OS-cyclin-A2-EGFP-Tet-Off inducible cell line was established as described previously (Theis-Febvre et al., 2003). Microinjection was performed into G1/S-synchronised cells (DNA) or mitotic cells (DQ-ovalbumin-647; O-34784, Invitrogen). The reagents used were: epoxomicin (4 μM; E3652, Sigma-Aldrich), bafilomycin A1 (0.5 μM; B1793, Sigma-Aldrich), Earle's balanced salts solution (E2888, Sigma-Aldrich) and puromycin (InvivoGen).

FLIM

FLIM was performed with a two-photon microscope, based on a Zeiss LSM510 Meta NLO with a Ti:Sapphire Chameleon-XR laser (Coherent), a fast hybrid photomultiplier (HPM-100-40) and SPC-830 time-correlated single-photon counting (TCSPC) electronics (Becker&Hickl). FLIM analysis was performed with SPCImage (Becker & Hickl) or TRI2 (Paul Barber, University of Oxford, UK).

Immunofluorescence

Cells were treated with paraformaldehyde (3.2%), Triton X-100 (0.5%) or with methanol-acetic acid. The following antibodies were used: anti-cyclin-A2 (clone 6E6, Novocastra Leica), anti-Cdc20 (Santa Cruz sc-8358), anti-LC3-B (L7543, Sigma-Aldrich), anti-p62 (sc-25575, Santa Cruz Biotechnology), FITC-conjugated goat anti-mouse-IgG (731853, Cell Lab) and Alexa-Fluor-555-conjugated goat anti-rabbit-IgG (Invitrogen). LysoTracker® Red DND-99 (L-7528, Invitrogen) was used to stain lysosomes, and Hoechst 33342 (Invitrogen) was used to stain DNA.

Immunoprecipitation and immunoblotting

Cells were lysed in NP-40 buffer containing 10 mM N-ethylmaleimide (E3876, Sigma-Aldrich) and 4 µM epoxomicin. Dynabeads (100-04D, Invitrogen) were pre-incubated with antibodies [anti-cyclin-A2 (sc-751, Santa Cruz Biotechnology), anti-LC3-B and anti-GFP (A11122, Invitrogen)]. The antibodies used for immunoblotting were anti-p62 (sc-28359, Santa Cruz), anti-Atg7 (A2856, Sigma-Aldrich), anti-LC3-B, anti-GAPDH (G9545, Sigma-Aldrich) and phospho-histone H3 (S10; #9701, Cell Signaling Technology).

Acknowledgements

We thank Maïté Coppey-Moisan (Institut Jacques Monod, Paris, France) for pmCherry vectors and Paul Barber (University of Oxford, UK) for TRI2 software. We thank Aude Echalier-Glazer (Centre de Biochimie Structurale, Montpellier, France) for the cyclin-A2-K5 mutant design. This work was possible thanks to Montpellier RIO Imaging facility. We are grateful to Vjekoslav Dulic and Robert Hipskind (Institut de Génétique Moléculaire de Montpellier, Montpellier, France) for helpful discussions.

Competing interests

The authors declare no competing interests.

Author contributions

A.L. performed most experiments. M.Z. and C.R. performed preliminary experiments. V.B. produced the U2OS-cyclin-A2-EGFP cell line. V.B. and O.C. contributed to UPS-related experiments. M.B.P. contributed to autophagy-related experiments. J.M.B. and M.P. supervised the project. M.P. wrote the manuscript.

Funding

This work was supported by the Agence Nationale de la Recherche [grant number 08-BLAN-0037-02], and the Fondation ARC pour la Recherche sur le Cancer. A.L. was supported by the Centre National de la Recherche Scientifique, the Région Languedoc-Roussillon and the Fondation pour la Recherche Médicale.

Supplementary material

Supplementary material available online at
http://jcs.biologists.org/lookup/suppl/doi:10.1242/jcs.139188/-/DC1

References

Arsic, N., Bendris, N., Peter, M., Begon-Pescia, C., Rebouissou, C., Gadéa, G., Bouquier, N., Bibeau, F., Lemmers, B. and Blanchard, J. M. (2012). A novel function for Cyclin A2: control of cell invasion via RhoA signaling. *J. Cell Biol.* **196**, 147-162.

Bailly, E., Pines, J., Hunter, T. and Bornens, M. (1992). Cytoplasmic accumulation of cyclin B1 in human cells: association with a detergent-resistant compartment and with the centrosome. *J. Cell Sci.* **101**, 529-545.

Baldin, V., Militello, M., Thomas, Y., Doucet, C., Fic, W., Boireau, S., Jariel-Encontre, I., Piechaczyk, M., Bertrand, E., Tazi, J. et al. (2008). A novel role for PA28gamma-proteasome in nuclear speckle organization and SR protein trafficking. *Mol. Biol. Cell* **19**, 1706-1716.

Bjørkøy, G., Lamark, T., Brech, A., Outzen, H., Perander, M., Overvatn, A., Stenmark, H. and Johansen, T. (2005). p62/SQSTM1 forms protein aggregates degraded by autophagy and has a protective effect on huntingtin-induced cell death. *J. Cell Biol.* **171**, 603-614.

Cardoso, M. C., Leonhardt, H. and Nadal-Ginard, B. (1993). Reversal of terminal differentiation and control of DNA replication: cyclin A and Cdk2 specifically localize at subnuclear sites of DNA replication. *Cell* **74**, 979-992.

den Elzen, N. and Pines, J. (2001). Cyclin A is destroyed in prometaphase and can delay chromosome alignment and anaphase. *J. Cell Biol.* **153**, 121-136.

Di Fiore, B. and Pines, J. (2010). How cyclin A destruction escapes the spindle assembly checkpoint. *J. Cell Biol.* **190**, 501-509.

Dulić, V., Stein, G. H., Far, D. F. and Reed, S. I. (1998). Nuclear accumulation of p21Cip1 at the onset of mitosis: a role at the G2/M-phase transition. *Mol. Cell. Biol.* **18**, 546-557.

Fung, T. K., Ma, H. T. and Poon, R. Y. (2007). Specialized roles of the two mitotic cyclins in somatic cells: cyclin A as an activator of M phase-promoting factor. *Mol. Biol. Cell* **18**, 1861-1873.

Geley, S., Kramer, E., Gieffers, C., Gannon, J., Peters, J. M. and Hunt, T. (2001). Anaphase-promoting complex/cyclosome-dependent proteolysis of human cyclin A starts at the beginning of mitosis and is not subject to the spindle assembly checkpoint. *J. Cell Biol.* **153**, 137-148.

Izawa, D. and Pines, J. (2011). How APC/C-Cdc20 changes its substrate specificity in mitosis. *Nat. Cell Biol.* **13**, 223-233.

Jackman, M., Kubota, Y., den Elzen, N., Hagting, A. and Pines, J. (2002). Cyclin A- and cyclin E-Cdk complexes shuttle between the nucleus and the cytoplasm. *Mol. Biol. Cell* **13**, 1030-1045.

Kallio, M., Weinstein, J., Daum, J. R., Burke, D. J. and Gorbsky, G. J. (1998). Mammalian p55CDC mediates association of the spindle checkpoint protein Mad2 with the cyclosome/anaphase-promoting complex, and is involved in regulating anaphase onset and late mitotic events. *J. Cell Biol.* **141**, 1393-1406.

Mateo, F., Vidal-Laliena, M., Canela, N., Busino, L., Martinez-Balbas, M. A., Pagano, M., Agell, N. and Bachs, O. (2009). Degradation of cyclin A is regulated by acetylation. *Oncogene* **28**, 2654-2666.

Morgan, D. O. (1997). Cyclin-dependent kinases: engines, clocks, and microprocessors. *Annu. Rev. Cell Dev. Biol.* **13**, 261-291.

Nishiyama, A., Tachibana, K., Igarashi, Y., Yasuda, H., Tanahashi, N., Tanaka, K., Ohsumi, K. and Kishimoto, T. (2000). A nonproteolytic function of the proteasome is required for the dissociation of Cdc2 and cyclin B at the end of M phase. *Genes Dev.* **14**, 2344-2357.

Pagano, M., Pepperkok, R., Verde, F., Ansorge, W. and Draetta, G. (1992). Cyclin A is required at two points in the human cell cycle. *EMBO J.* **11**, 961-971.

Pankiv, S., Clausen, T. H., Lamark, T., Brech, A., Bruun, J. A., Outzen, H., Øvervatn, A., Bjørkøy, G. and Johansen, T. (2007). p62/SQSTM1 binds directly to Atg8/LC3 to facilitate degradation of ubiquitinated protein aggregates by autophagy. *J. Biol. Chem.* **282**, 24131-24145.

Pascreau, G., Eckerdt, F., Churchill, M. E. and Maller, J. L. (2010). Discovery of a distinct domain in cyclin A sufficient for centrosomal localization independently of Cdk binding. *Proc. Natl. Acad. Sci. USA* **107**, 2932-2937.

Peter, M. and Ameer-Beg, S. M. (2004). Imaging molecular interactions by multiphoton FLIM. *Biol. Cell* **96**, 231-236.

Peter, M., Ameer-Beg, S. M., Hughes, M. K., Keppler, M. D., Prag, S., Marsh, M., Vojnovic, B. and Ng, T. (2005). Multiphoton-FLIM quantification of the EGFP-mRFP1 FRET pair for localization of membrane receptor-kinase interactions. *Biophys. J.* **88**, 1224-1237.

Pines, J. and Hunter, T. (1991). Human cyclins A and B1 are differentially located in the cell and undergo cell cycle-dependent nuclear transport. *J. Cell Biol.* **115**, 1-17.

Rockel, T. D., Stuhlmann, D. and von Mikecz, A. (2005). Proteasomes degrade proteins in focal subdomains of the human cell nucleus. *J. Cell Sci.* **118**, 5231-5242.

Seeger, M., Hartmann-Petersen, R., Wilkinson, C. R., Wallace, M., Samejima, I., Taylor, M. S. and Gordon, C. (2003). Interaction of the anaphase-promoting complex/cyclosome and proteasome protein complexes with multiubiquitin chain-binding proteins. *J. Biol. Chem.* **278**, 16791-16796.

Sobczak-Thepot, J., Harper, F., Florentin, Y., Zindy, F., Brechot, C. and Puvion, E. (1993). Localization of cyclin A at the sites of cellular DNA replication. *Exp. Cell Res.* **206**, 43-48.

Sudakin, V., Ganoth, D., Dahan, A., Heller, H., Hershko, J., Luca, F. C., Ruderman, J. V. and Hershko, A. (1995). The cyclosome, a large complex containing cyclin-selective ubiquitin ligase activity, targets cyclins for destruction at the end of mitosis. *Mol. Biol. Cell* **6**, 185-197.

Tanida, I., Tanida-Miyake, E., Ueno, T. and Kominami, E. (2001). The human homolog of Saccharomyces cerevisiae Apg7p is a Protein-activating enzyme for multiple substrates including human Apg12p, GATE-16, GABARAP, and MAP-LC3. *J. Biol. Chem.* **276**, 1701-1706.

Theis-Febvre, N., Filhol, O., Froment, C., Cazales, M., Cochet, C., Monsarrat, B., Ducommun, B. and Baldin, V. (2003). Protein kinase CK2 regulates CDC25B phosphatase activity. *Oncogene* **22**, 220-232.

Thomas, Y., Coux, O. and Baldin, V. (2010). βTrCP-dependent degradation of CDC25B phosphatase at the metaphase-anaphase transition is a pre-requisite for correct mitotic exit. *Cell Cycle* **9**, 4338-4350.

Tramier, M., Zahid, M., Mevel, J. C., Masse, M. J. and Coppey-Moisan, M. (2006). Sensitivity of CFP/YFP and GFP/mCherry pairs to donor photobleaching on FRET determination by fluorescence lifetime imaging microscopy in living cells. *Microsc. Res. Tech.* **69**, 933-939.

Walker, A., Acquaviva, C., Matsusaka, T., Koop, L. and Pines, J. (2008). UbcH10 has a rate-limiting role in G1 phase but might not act in the spindle checkpoint or as part of an autonomous oscillator. *J. Cell Sci.* **121**, 2319-2326.

Wolthuis, R., Clay-Farrace, L., van Zon, W., Yekezare, M., Koop, L., Ogink, J., Medema, R. and Pines, J. (2008). Cdc20 and Cks direct the spindle checkpoint-independent destruction of cyclin A. *Mol. Cell* **30**, 290-302.

Yamamoto, A., Tagawa, Y., Yoshimori, T., Moriyama, Y., Masaki, R. and Tashiro, Y. (1998). Bafilomycin A1 prevents maturation of autophagic vacuoles by inhibiting fusion between autophagosomes and lysosomes in rat hepatoma cell line, H-4-II-E cells. *Cell Struct. Funct.* **23**, 33-42.

Yoshimori, T., Yamamoto, A., Moriyama, Y., Futai, M. and Tashiro, Y. (1991). Bafilomycin A1, a specific inhibitor of vacuolar-type H(+)-ATPase, inhibits acidification and protein degradation in lysosomes of cultured cells. *J. Biol. Chem.* **266**, 17707-17712.